

## Supplementary Information

### **Copper Phthalocyanine Modified Hydrogel Inverse Opal Beads for Enhanced Photocatalytic Removal of Dyes**

Fengtong Shen,<sup>a</sup> Jingzhen Wang,<sup>a</sup> Libin Wang,<sup>a</sup> Linlin Zang<sup>\*b</sup> Qing Xu,<sup>a</sup> Liguao Sun<sup>\*a</sup>  
and Yanhong Zhang<sup>\*a</sup>

<sup>a</sup> School of Chemical Engineering and Materials, Heilongjiang University, Harbin,  
150080, P. R. China. Tel: +86-152-4503-2548; +86-158-4658-9441

E-mail: sunliguo1975@163.com; zhangyanhong1996@163.com

<sup>b</sup> School of Environmental Science and Engineering, Southern University of Science  
and Technology, Shenzhen 518055, P. R. China.

E-mail: zangll423@163.com

## **1. Experimental section**

### **1.1. Materials**

Silica nanoparticles with an average diameter of about 285 nm were prepared according to previous study.<sup>1</sup> Dimethyl silicone oil was supplied by Guangfu Chemicals Ltd. Acrylic acid (AAc), N, N'-methylenebisacrylamide (MBA), 2-hydroxy-2-methylpropiophenone (HMPP),  $\beta$ -copper (II) phthalocyanine (CuPc) and all dyes were obtained from Aladdin Chemical Reagent Co., Ltd. Ethanol, acrylamide (AAm) and n-hexane were purchased from Sinopharm Chemical Reagent Co., Ltd. All chemical reagents were of analytical grade and used directly without purification.

### **1.2. Preparation of silica nanoparticles**

Silica nanoparticles were synthesized by a modified Stober method. Briefly, 3 mL of TEOS was added dropwise to a mixture solution containing 100 mL of ethanol, 2.0 mL of deionized (DI) water, and 4.5 mL of ammonia (25%), followed by stirring at 40 °C for 4 h. Afterwards, an additional 2.0 mL of TEOS was added to the solution and stirred for 12 h. After the reaction, the mixture was purified by centrifugation to obtain 285 nm silica nanoparticles.

### **1.3. Preparation of silica colloidal crystal beads (SCCBs)**

According to the reported literature,<sup>2,3</sup> a modified microfluidic technique was utilized to fabricate silica colloidal crystal beads (SCCBs). Typically, silica nanoparticles were dispersed in DI water to prepare a 20 wt.% suspension. Two syringes filled with 10 mL of suspension and 100 mL of dimethyl silicone oil were loaded onto a microfluidic syringe pump. Among them, the pushing speeds of the

suspension as the dispersed phase and oil as the continuous phase were set to 0.4 and 65 mL h<sup>-1</sup>, respectively. Under the shear force, silica droplets were formed at the junction of the T-shaped channel, and then received by a polypropylene container filled with dimethyl silicone oil. They were transferred to a vacuum oven and dried at 60 °C for 12 h. The resulting beads were repeatedly washed by n-hexane to remove the silicone oil. Finally, the SCCBs were obtained by calcination at 750 °C for 4 h.

#### **1.4. Preparation of PACA hydrogel inverse opal beads (PACA HIOBs)**

In this study, hydrogel beads with inverse opal structures were obtained by a sacrificial template method. First, AAm monomer (0.45 g), AAc monomer (0.45 g), MBA crosslinker (0.1 g), HMPP photo-initiator (60 µL), and DI water (2.33 mL) were mixed into a casting solution, followed by soaking SCCBs in the solution for 2 h. After UV polymerization for 20 min, SCCBs was removed with 4 M ammonium bifluoride, and the residual solvent was washed with DI water to obtain PACA HIOBs.

#### **1.5. Preparation of CuPc modified PACA HIOBs (CuPc-PACA HIOBs)**

50 mg of PACA HIOBs was immersed in 50 mL of 20 mg L<sup>-1</sup> CuPc ethanol solution and stirred gently for 5 min, and then soaked in deionized water for 2 min. After repeating the above steps for 1 to 5 times, CuPc-PACA HIOBs containing different CuPc loadings (0~1.058 wt.%) were obtained. In the experiment, the concentration and mass of residual CuPc in the solution were analyzed using a UV-Vis spectrophotometer. The detailed experimental parameters were provided in Table S1.

Table S1. The preparation parameters of the CuPc-PACA HIOBs with different CuPc

contents. The initial concentration of the CuPc in 50 mL of ethanol was 20 mg L<sup>-1</sup>, and the mass of PACA HIOBs was 50 mg.

Samples	Soaking times	Residual concentration of CuPc after soaking (mg L <sup>-1</sup> )	Residual mass of CuPc after soaking (mg)	Total loading mass of CuPc (mg)	Content of CuPc (wt.%)
0 wt.% (PACA HIOBs)	0	-	-	0	0
0.314 wt.%	1	16.868	0.843	0.157	0.314
0.590 wt.%	2	17.202	0.860	0.297	0.590
0.808 wt.% (CuPc-PACA HIOBs)	3	17.804	0.890	0.407	0.808
0.962 wt.%	4	18.420	0.921	0.486	0.962
1.058 wt.%	5	19.022	0.951	0.535	1.058

## 1.6. Characterization

The morphology and structure of the samples were characterized by TESCAN MIRA LMS scanning electron microscope (SEM) and JEOL JEM-2100 transmission electron microscope (TEM). The element composition of the samples was analyzed by energy dispersive spectrometer (EDS, OXFORD instrument). Optical images were recorded with a stereo microscope (Olympus SZ61TR) equipped with a camera (Canon EOS500D). N<sub>2</sub> adsorption-desorption were measured by ASAP 2460 (Micrometrics). Fourier transform infrared spectroscopy (FTIR) was acquired on a Perkin-Elmer Spectrum One instrument. XRD analysis was performed on an X-ray spectrometer (D8 ADVANCE, Cu K $\alpha$  radiation ( $\lambda=1.5406$  Å)). The elemental composition and chemical state of all samples was confirmed using X-ray photoelectron spectroscopy (XPS) from

the Thermo Fisher Scientific K-Alpha. UV-Vis diffuse reflectance spectra (DRS) were obtained using a Perkin-Elmer Lambda 950 UV-Vis spectrophotometer. The photoluminescence (PL) spectra of the as-prepared samples were revealed on a fluorescence spectrophotometer (Hitachi, F-4600) at an excitation wavelength of 450 nm. Electrochemical impedance spectroscopy (EIS) and transient photocurrent response were performed on an electrochemical workstation (Chenhua CHI 760E).

### **1.7. Evaluation of photocatalytic performance**

Different organic dyes (e.g., Rhodamine B, Malachite green, Methyl orange, Reactive red X-3B, Reactive black 5, Remazol Brilliant Blue R) were chosen as target pollutants to evaluate the photodegradation performance of the CuPc-PACA HIOBs. Typically, photocatalytic experiments were carried out in a 250 mL sealed quartz reaction equipped with circulating cooling water. Before turning on the light source, the reaction system cell containing 50 mg of CuPc-PACA HIOBs and 100 mL of dyes ( $10 \text{ mg L}^{-1}$ ) was placed in the dark for 30 min to reach adsorption equilibrium. Then, a 300 W xenon lamp (PLS-SXE300/300UV, Perfect Light) was used as the light source. A certain volume of the reaction solution was collected with a syringe at regular intervals, and then the concentration of the dye was determined by a UV-visible spectrophotometer (TU-1901, Beijing Purkinje GENERAL Instrument). Five cycles of catalytic experiments were performed to evaluate the reusability and stability of the catalysts. Before each cycle, the dye solution was added to the reactor without adding additional catalyst.

## 2. Results and Discussion

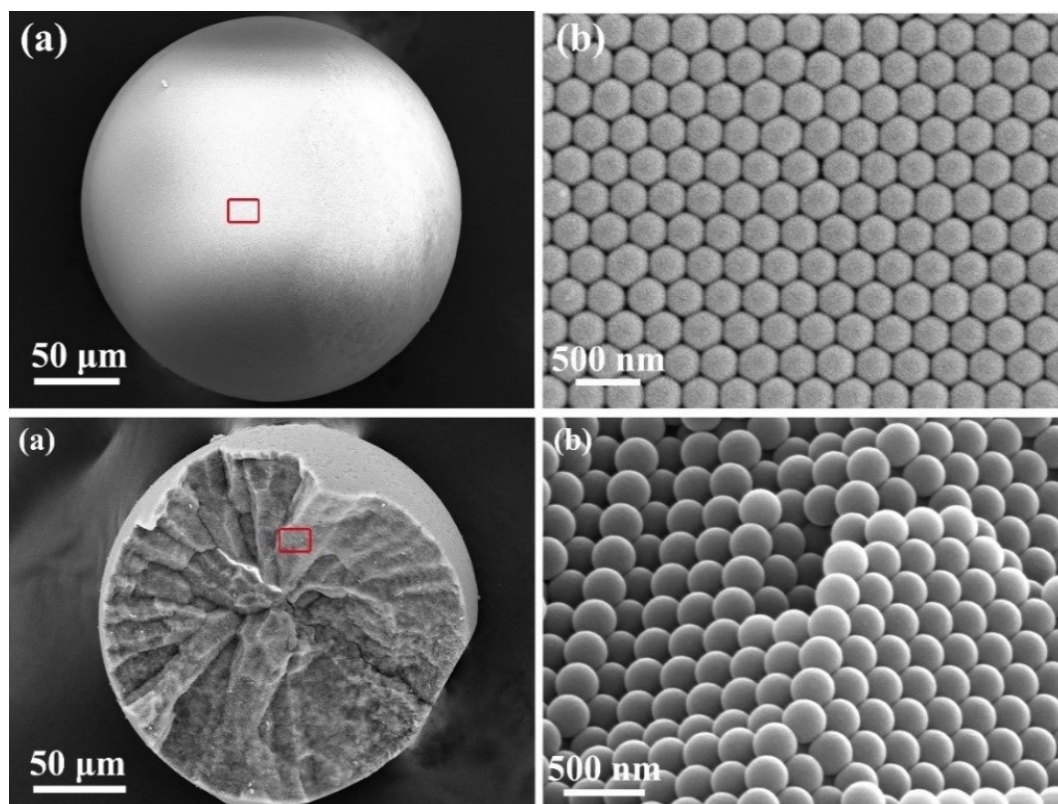


Fig. S1. (a-d) SEM images of the SCCBs.

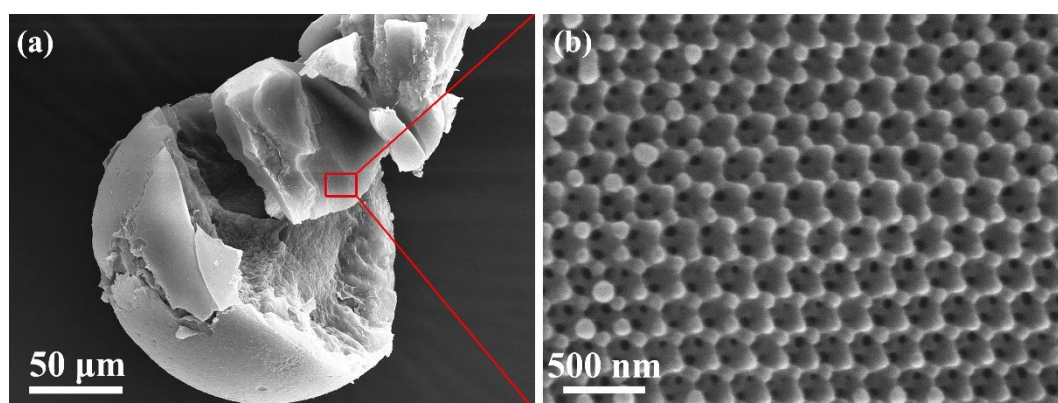


Fig. S2. SEM images of the inner morphology of the PACA HIOBs.

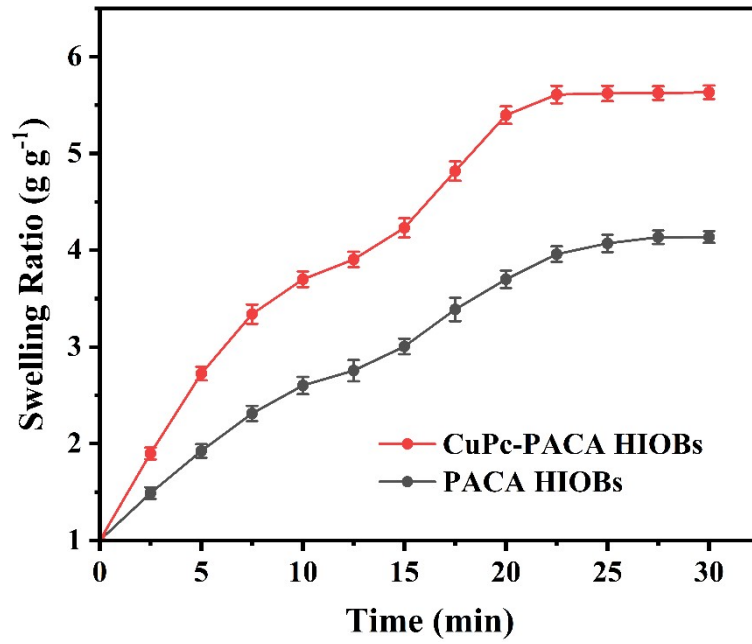


Fig. S3. The swelling rate of the PACA HIOBs and CuPc-PACA HIOBs.

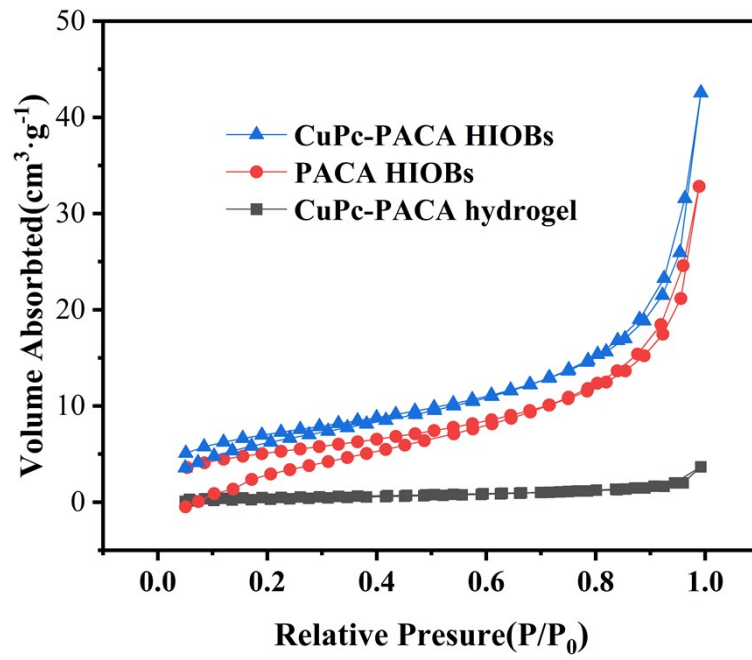


Fig. S4. N<sub>2</sub> adsorption-desorption isotherms CuPc-PACA hydrogel, PACA HIOBs and CuPc-PACA HIOBs.

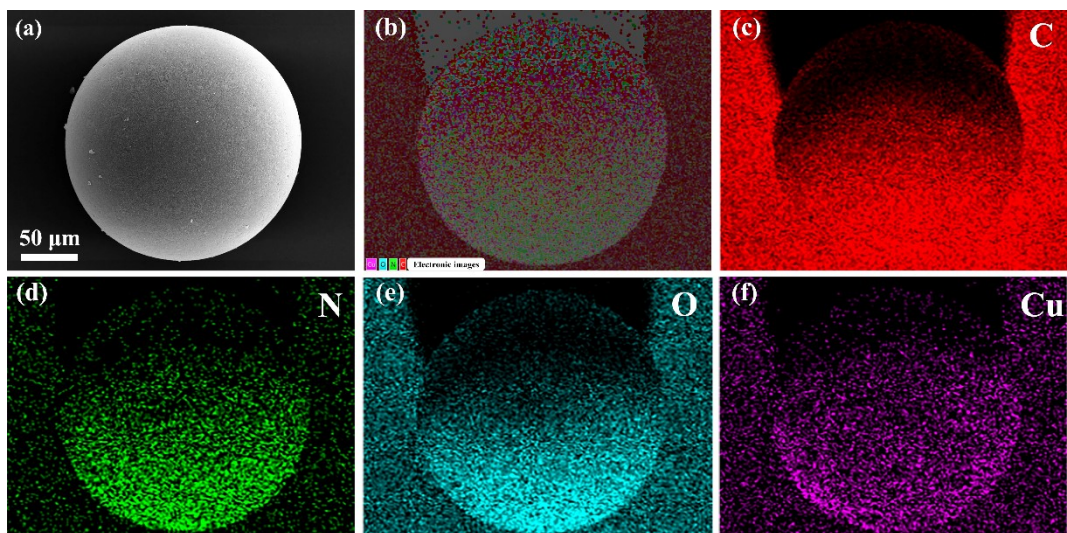


Fig. S5. SEM-EDS elemental mapping of CuPc-PACA HIOBs.

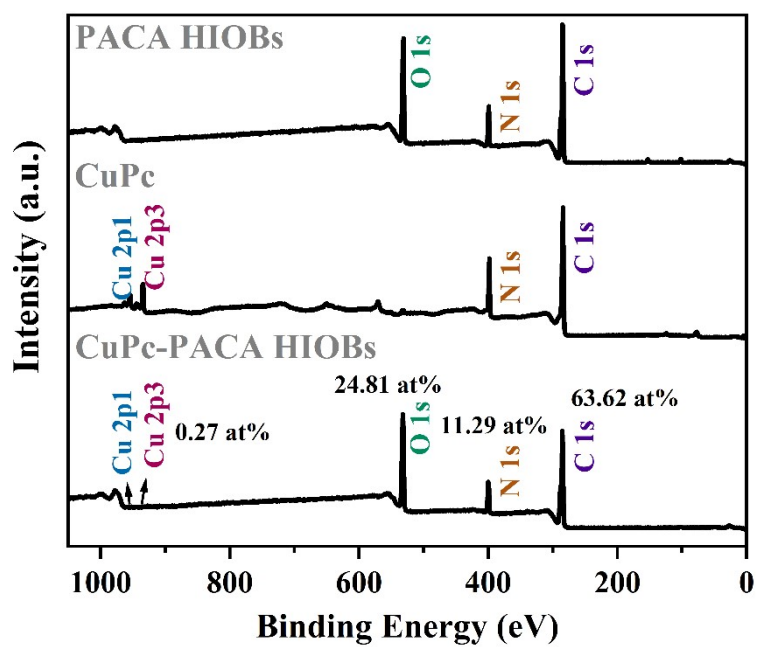


Fig. S6. Wide XPS survey spectra of the PACA HIOBs, CuPc and CuPc-PACA HIOBs.



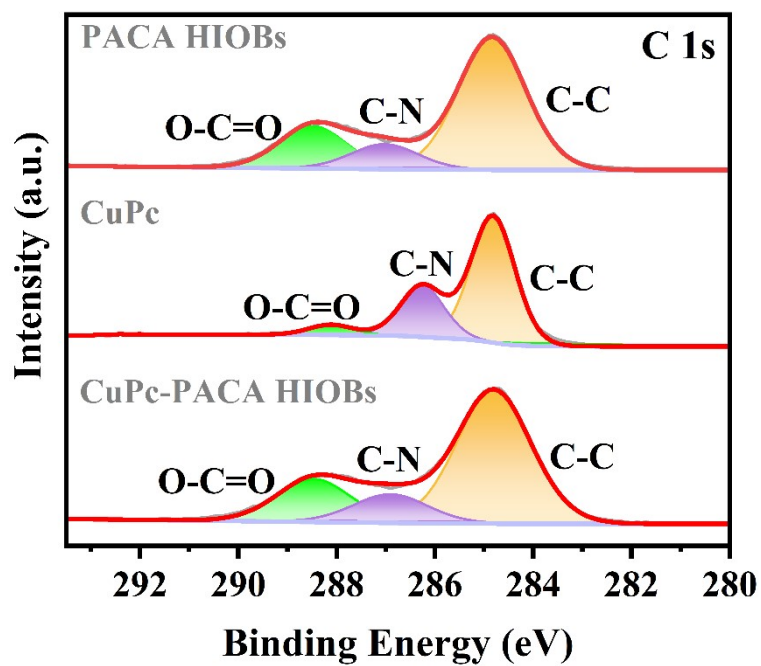


Fig. S7. C 1s HRXPS spectra of the PACA HIOBs, CuPc, and CuPc-PACA HIOBs.

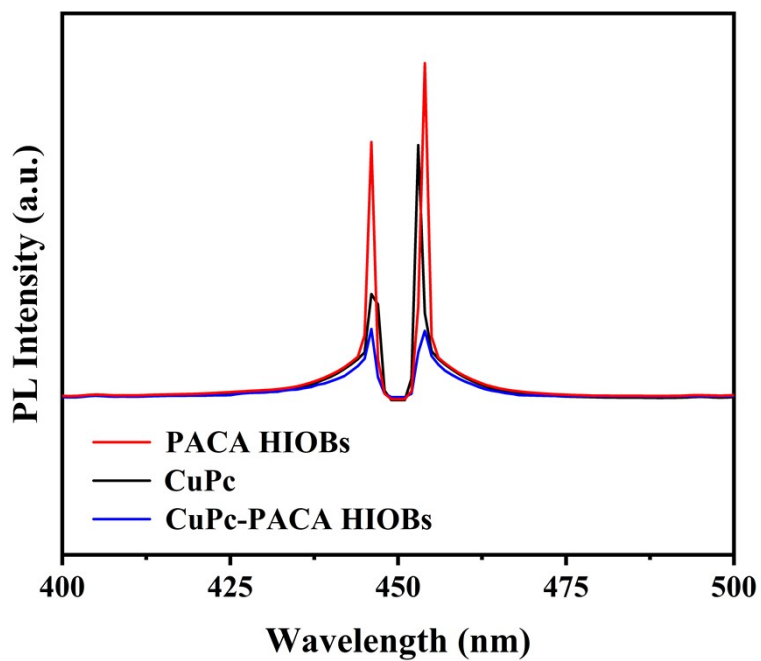


Fig. S8. PL spectra of the CuPc, PACA HIOBs and CuPc-PACA HIOBs.

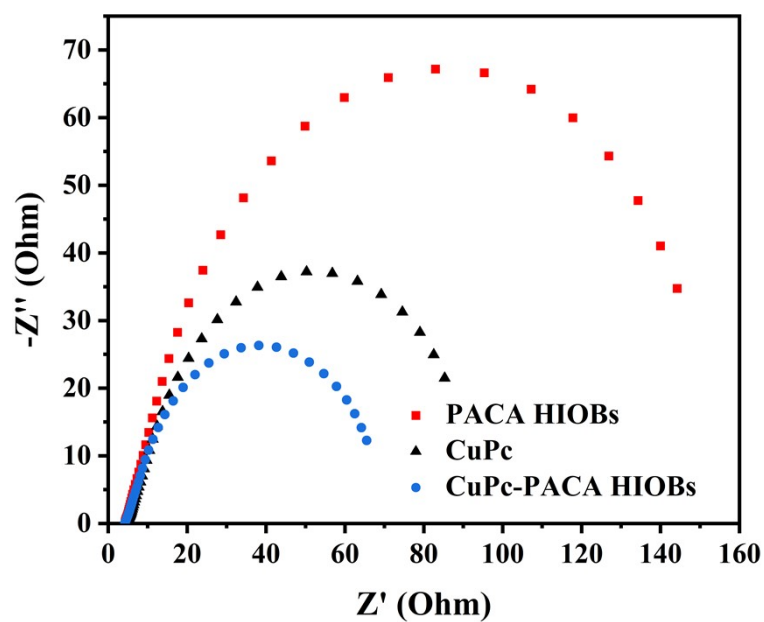


Fig. S9. EIS Nyquist plots of the CuPc, PACA HIOBs and CuPc-PACA HIOBs.

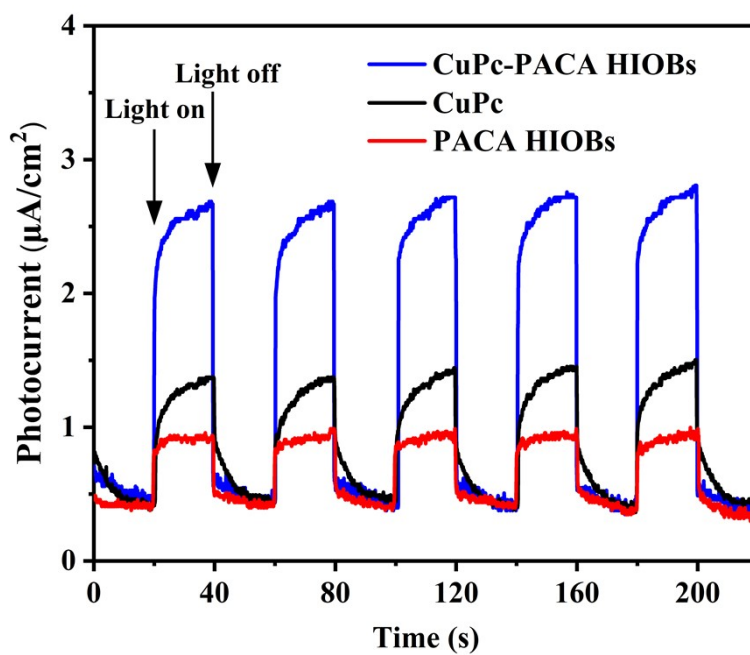
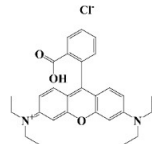
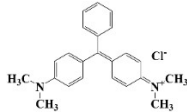
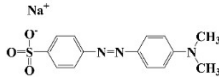
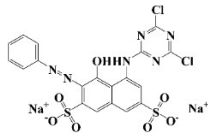
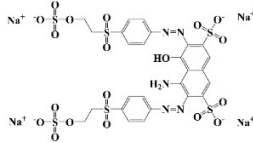
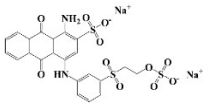


Fig. S10. Transient photocurrent response curves of the CuPc, PACA HIOBs and CuPc-PACA HIOBs.

Table S2. The structure and properties of various dyes.

Dye	Class	Molecular formula	Relative molecular mass	$\lambda_{max}$ (nm)	Structural formula	Removal rate	Illumination time (min)
Rhodamine B	Xanthene dyes	$C_{28}H_{31}ClN_2O_3$	479.01	553.5		~100%	40
Malachite green	Triphenylmethane dyes	$C_{23}H_{25}ClN_2$	364.92	617		98.1%	30
Methyl orange	Azo dyes	$C_{14}H_{14}N_3NaO_3S$	327.33	463		97.9%	17
Reactive red X-3B	X-type reactive dyes	$C_{19}H_{10}Cl_2N_6Na_2O_7S_2$	615.33	537.5		~100%	15
Reactive black 5	Double azo dyes	$C_{26}H_{21}N_5Na_4O_{19}S_6$	991.82	597.5		~100%	20
Remazol Brilliant Blue R	Anthraquinone dyes	$C_{22}H_{16}N_2Na_2O_{11}S_3$	626.54	588.5		94.3%	40

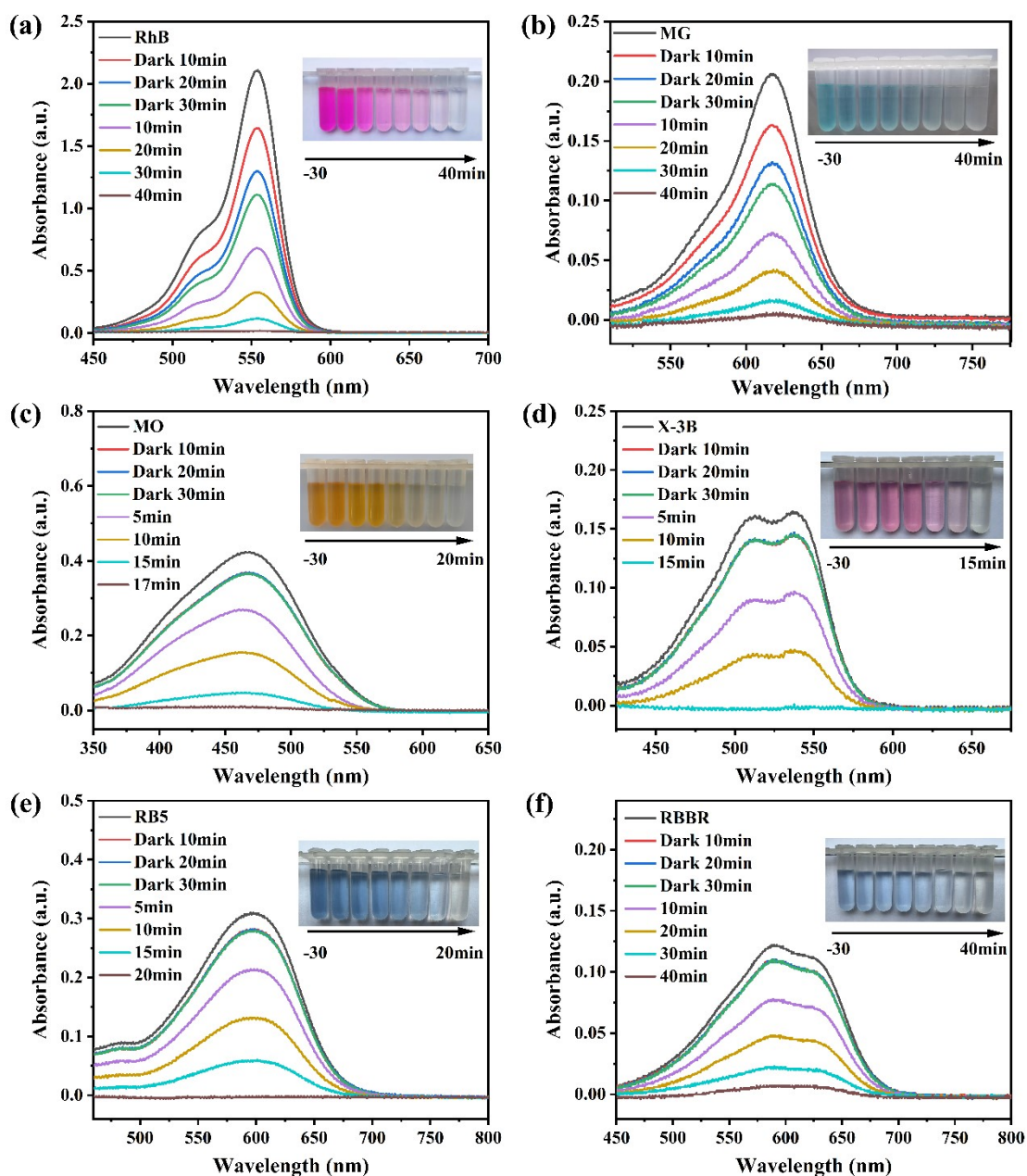


Fig. S11. The UV-vis absorption spectra of different dyes solution as a function of reaction time when the CuPc-PACA HIOBs were used as the photocatalyst: (a) RhB, (b) MG, (c) MO, (d) X-3B, (e) RB5, and (f) RBBR. Inserted digital photos represented color changes of the dye wastewater at different time intervals.

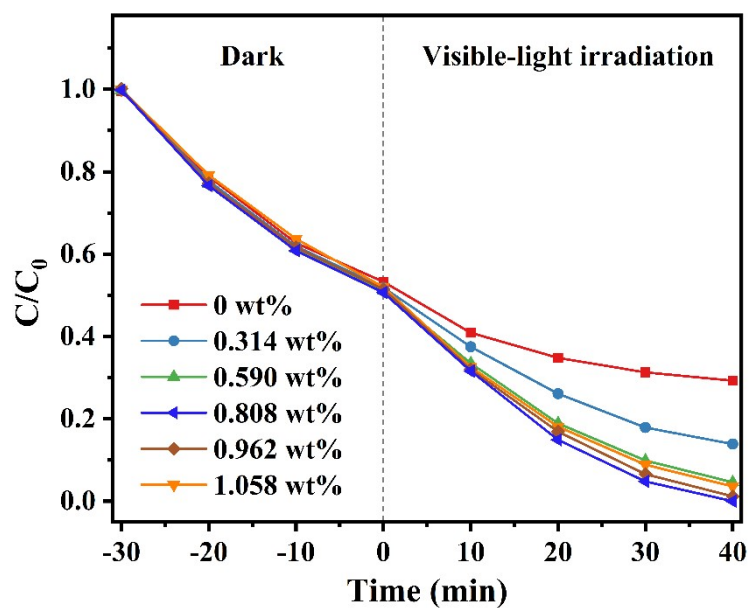


Fig. S12. The effect of the CuPc loading mass on the photodegradation performance of the RhB.

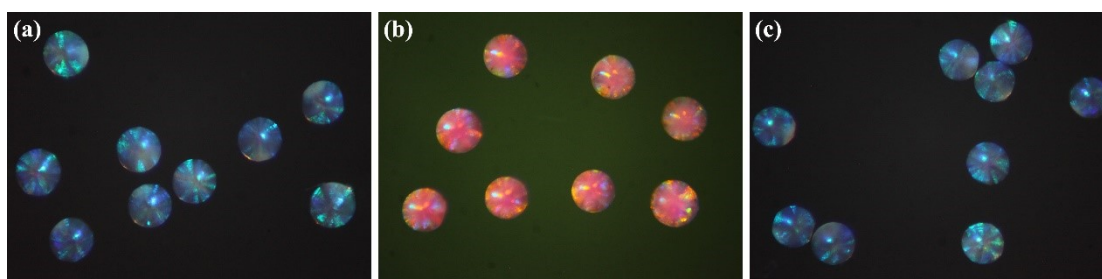


Fig. S13. Optical images of the CuPc-PACA HIOBs at different stages of photocatalytic degradation reaction.

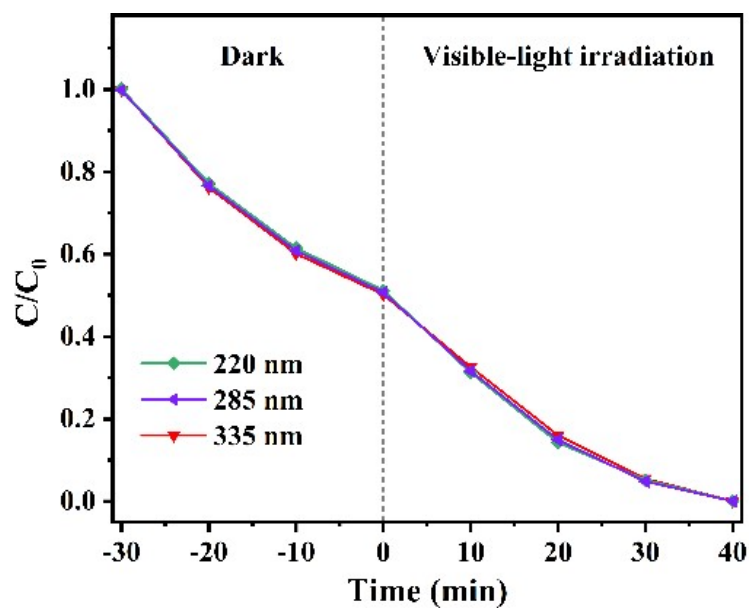


Fig. S14. Adsorption and photocatalytic degradation process of RhB by CuPc-PACA HIOBs with different pore sizes.

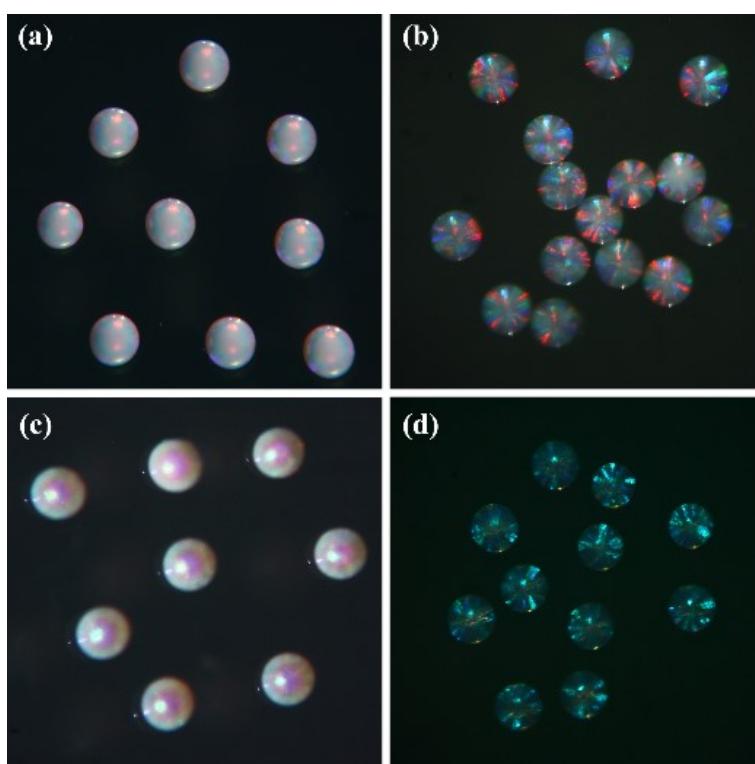


Fig. S15. Microscopic photographs of photonic crystals: (a) SCCBs (with 335nm silica), (b) corresponding CuPc-PACA HIOBs; (c) SCCBs (with 220nm silica) and (d) corresponding CuPc-PACA HIOBs.

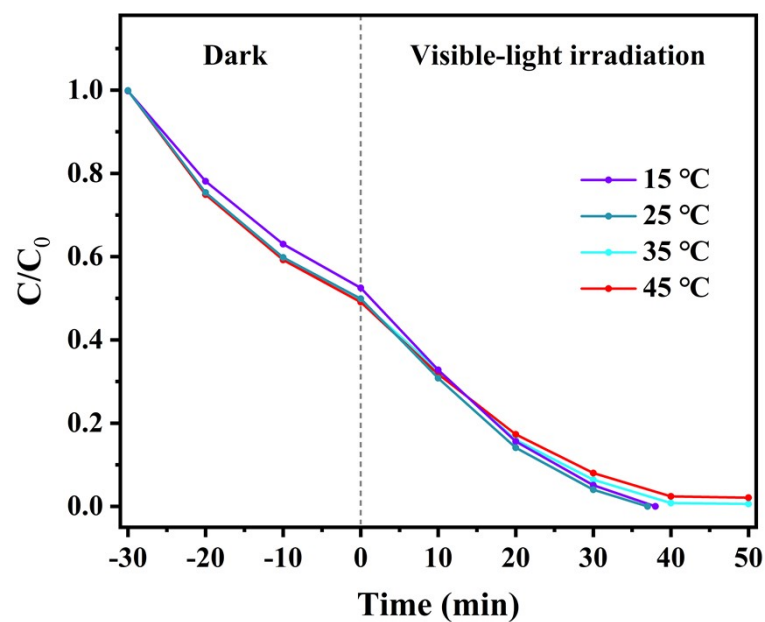


Fig. S16. Effect of different temperature on the degradation of RhB by CuPc-PACA HIOBs (Catalyst dosage: 50 mg,  $C_{\text{RhB}}$ :10 mg/L, pH=6.26).

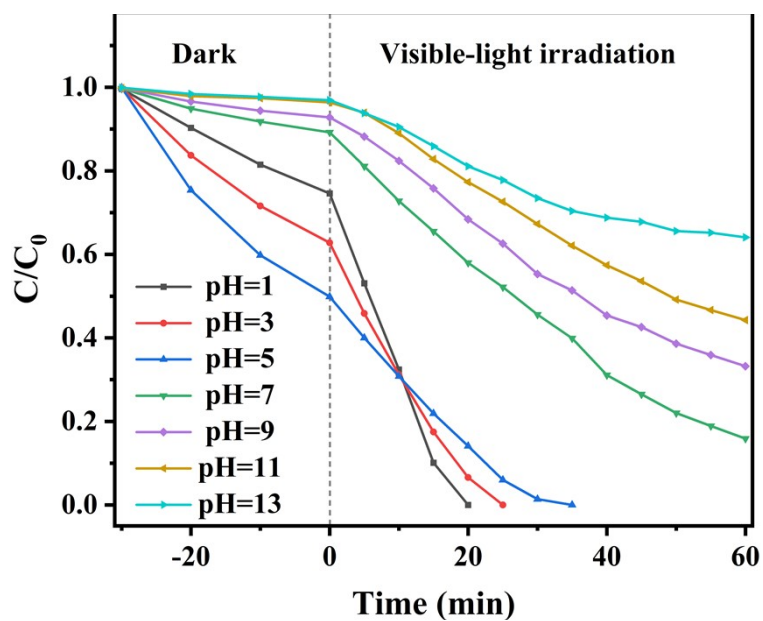


Fig. S17. Effect of different pH on the degradation of RhB by CuPc-PACA HIOBs (Catalyst dosage: 50 mg,  $C_{\text{RhB}}$ :10 mg L<sup>-1</sup>, Temperature: 25 °C).

Table S3. Comparison of degradation of dyes by CuPc and hydrogel-based photocatalysts.

Catalyst	Dye	Dosage	Volume and concentration	Removal rate	$k$ (min <sup>-1</sup> )
Cr <sub>2</sub> O <sub>3</sub> /La <sub>2</sub> Ti <sub>2</sub> O <sub>7</sub>	X-3B	-	-	-	0.075
Cu <sub>2</sub> O/TiO <sub>2</sub>	X-3B	100 mg	200 mL, 25 mg L <sup>-1</sup>	81.20%	0.0299
Sm <sub>2</sub> Ti <sub>2</sub> O <sub>7</sub> /HZSM	X-3B	20 mg	50 mL, 30 mg L <sup>-1</sup>	-	0.0172
KNbO <sub>3</sub> /ZnO	MO	100 mg	100 mL, 10 ppm	-	0.0470
TiO <sub>2</sub> -TOCN-PAM	MO	2000 mg	40 mL, 10 mg L <sup>-1</sup>	97.3%	0.0425
CoZnO/PVA	MO	-	-	100%	0.025
TiO <sub>2</sub> /GMAC	RB5	-	-	-	0.024
Fe <sup>3+</sup> @ZnO PMR	RB5	-	-, 30 ppm	88.89%	0.014
La-doped CTO	RB5	-	-, 20 ppm	85.6%	0.0094
Ag/AgCl-CMC	RhB	280 mg	70 mL, 10 ppm	98%	0.052
RGO/CuPc	RhB	15 mg	120 mL, 5×10 <sup>-6</sup> M	96.2%	0.0143
Char-Ni-PAA hydrogels	RhB	5000 mg	100 mL, 10 ppm	75.56%	0.0033
FNZP/PAM	MG	0.25 mg mL <sup>-1</sup>	10 <sup>-6</sup> M	97.45%	0.052
ZnO/N, S-CQDs	MG	10 mg	25 mL, 2×10 <sup>-5</sup> M	85.4%	0.0292
GG/AO	MG	100 mg	1.5×10 <sup>-5</sup> M	90%	0.0189
CS TiO <sub>2</sub>	RBBR	100 mg	100 mL, 50mg L <sup>-1</sup>	-	0.0138
Ce <sub>0.95</sub> Mo <sub>0.15</sub> V <sub>0.85</sub> O <sub>4</sub>	RBBR	-	-, 40 ppm	100%	0.0091
ZrO <sub>2</sub>	RBBR	-	-, 25 ppm	~100%	0.0041
	<b>X-3B</b>			<b>100%</b>	<b>0.1218</b>
	<b>RB5</b>			<b>100%</b>	<b>0.0772</b>
<b>This work</b>	<b>MO</b>	<b>50 mg</b>	<b>100 mL, 10 mg L<sup>-1</sup></b>	<b>97.9%</b>	<b>0.0850</b>
	<b>RhB</b>			<b>100%</b>	<b>0.0685</b>
	<b>MG</b>			<b>98.1%</b>	<b>0.0601</b>
	<b>RBBR</b>			<b>94.3%</b>	<b>0.0461</b>



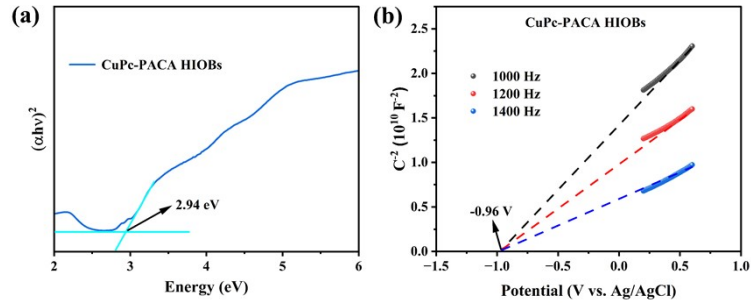


Fig. S18. (a) Band gap energy plots of CuPc-PACA HIOBs and (b) Mott-Schottky curves of CuPc-PACA HIOBs at different frequency.

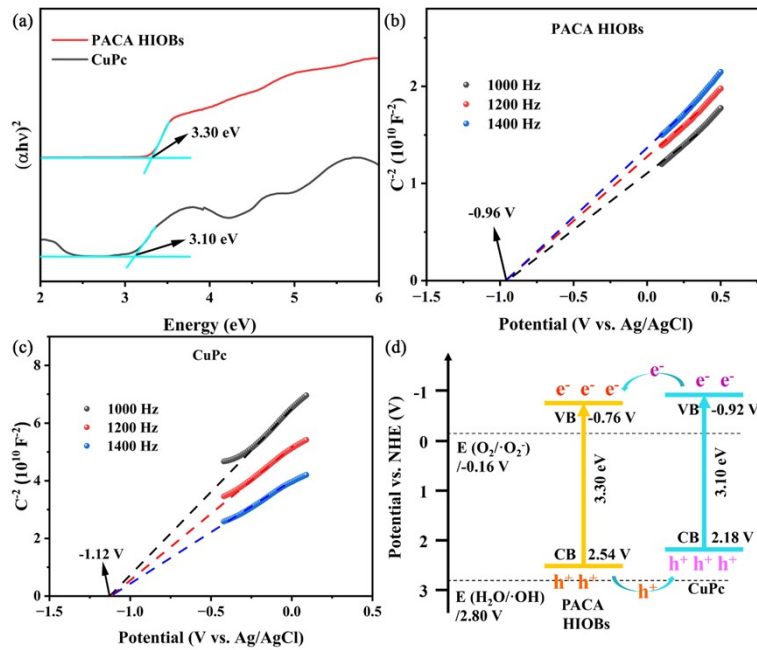


Fig. S19. (a) Band gap energy plots of CuPc and PACA HIOBs, (b,c) Mott-Schottky curves of PACA HIOBs and CuPc at different frequency and (d) band gap structure plots of CuPc and PACA HIOBs.

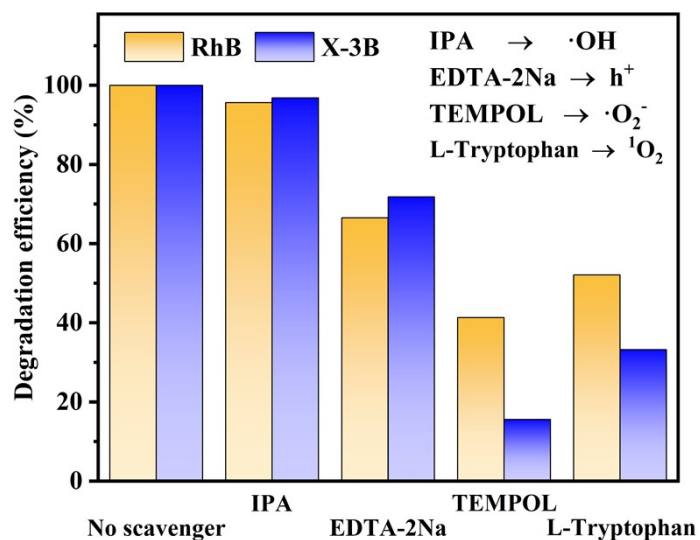


Fig. S20. Effects of different scavengers on the degradation efficiency of CuPc-PACA HIOBs.

## References

- 1 H. Giesche, *J. Eur. Ceram. Soc.*, 1994, **14**, 189–204.
- 2 L. Zang, X. Cao, Y. Zhang, L. Sun, C. Qin and C. Wang, *J. Mater. Chem. A*, 2015, **3**, 22088–22093.
- 3 X. Cao, L. Zang, Z. Bu, L. Sun, D. Guo and C. Wang, *J. Mater. Chem. A*, 2016, **4**, 10479–10485.